# ANOMALOUS CREEP IN SN-RICH SOLDER JOINTS

Ho Geon Song[1], John W. Morris, Jr.[1] and Fay Hua[2]
[1]Department of Materials Science and Engineering, University of California, Berkeley, CA 94720, USA
and Center for Advanced Materials, Lawrence Berkeley National Laboratory
[2]Materials Technology Operation, Intel Corporation,
Santa Clara, CA 95054, USA

## ABSTRACT

This paper discusses the creep behavior of example Sn-rich solders that have become candidates for use in Pb-free solder joints. The specific solders discussed are Sn-3.5Ag, Sn-3Ag-0.5Cu, Sn-0.7Cu and Sn-10In-3.1Ag, used in thin joints between Cu and Ni/Au metallized pads. The creep behavior of these joints was measured over the range 60-130°C. The four solders show the same general behavior. At all temperatures their steady-state creep rates are separated into two regimes with different stress exponents (n). The low-stress exponents range from ~3-6, while the high-stress exponents are anomalously high (7-12). Strikingly, the high-stress exponent has a strong temperature dependence near room temperature, increasing significantly as the temperature drops from 95 to 60°C. The anomalous behavior of the solders appears to be due to the dominant Sn constituent. Joints of pure Sn have stress exponents, n, that change with stress and temperature almost exactly like those of the Sn-rich solder joints. Surprisingly, however, very similar behavior is found in Sn-10In-3.1Ag, whose primary constituent is γ-InSn. Research on creep in bulk samples of pure Sn suggests that the anomalous temperature dependence of the stress exponent is due to a change in the dominant mechanism of creep. Whatever its source, it has the consequence that conventional constitutive relations for steady-state creep must be used with caution in treating Sn-rich solder joints, and qualification tests that are intended to verify performance should be carefully designed.

Keywords: creep behavior, tin-rich solder alloy, lead-free solder joints

## I. Introduction

Legislative and marketing pressures from many sources are forcing the gradual adoption of Pb-free solders in microelectronics. The design of reliable joints with these Pb-free solders is a formidable problem, given the lack of prior service experience and the shortage of probative mechanical property data.

A primary cause of service failures in solder joints is thermal fatigue. When an electronic device is turned on or off, or its internal circuits are activated, the soldered joints are heated or cooled. The joints are mechanically stressed in each thermal cycle because of inhomogeneous heating and differences in the thermal expansion coefficients of the various components. The dominant stresses tend to be in shear. Since the typical operating temperatures of microelectronic devices are a significant fraction of the melting temperatures of the solders used, the mechanical response to thermal stress is ordinarily high-temperature creep. Cyclic creep causes mechanical damage, and joints eventually fail by creep fatigue [1,2]. It follows that the understanding of creep behavior and creep mechanisms is fundamental to the design of reliable joints.

Many of the solder compositions that are attracting the greatest current interest are Sn-rich compositions from the Sn-Ag and Sn-Cu systems [3]. There is very little creep data for these compounds, and a good part of that which is available was measured with bulk samples whose relevance to the behavior of solder joints is not at all clear. Our own recent work, including that reported here, was intended to address this problem by conducting high-temperature creep tests on well-characterized solder joints. In this paper we shall discuss recent results with Sn-3.5Ag, Sn-3Ag-0.5Cu, Sn-0.7Cu and Sn-10In-3.1Ag (wt. %), made as thin joints connecting Cu and Ni/Au metallized substrates. As we shall see, the behavior of the Sn-Ag-Cu systems is strongly influenced by the dominant Sn phase. The Sn-10In-3.1Ag solder is very different in its microstructure, being a mixture of intermetallic phases, but, nonetheless, has a creep behavior that is similar to that of the Sn-Ag-Cu solders over the temperature range tested. Elsewhere, we have reported recent research on the Au-Sn [4], Sn-Bi and In-Sn [5] Pb-free solders.

## II. Experimental Procedure

The solder compositions discussed here were made by melting 20g ingots from pure (99.999) elemental starting materials. The Sn-0.7Cu, Sn-3Ag-0.5Cu and Sn-10In-3.1Ag (wt.%) alloys were made by vacuum arc melting. The Sn-3.5Ag alloy was melted in a vacuum-sealed quartz tube. The mass loss during melting was below 0.05g for the initial weight of 20g. After melting, the alloys were homogenized for 55hrs at 180°C, then cold rolled into foils of about 155 μm thickness.

The samples used in the creep tests were nine-pad single shear creep specimens with the geometry shown in Fig. 1. The substrate pad size is about 1.22mm x 2.24mm. The joints were made between dissimilar substrates (as is common in industrial practice); the pad metallization on one side was Cu while that on the other side was about 4 μm electroless Ni coated with about 0.13 μm immersion Au. The solder joint thickness was fixed at 160 μm. The shear specimens were reflowed in nitrogen with a peak temperature of 235°C for Sn-3.5Ag, Sn-3Ag-0.5Cu, and Sn-10In-3.1Ag and 245°C for Sn-0.7Cu.

Samples were cooled at the rate of 2.7°C/sec. (air cooling). In addition, some samples were cooled at the rate of 3.5°C/min. (furnace cooling) and tested at 130°C. After reflow the samples were aged at 160°C for 4 hours.

Creep tests were done in a dead-load creep machine (Fig. 2). The sample is loaded with a fixed weight while its temperature is controlled by an oil bath. The creep specimen is held by frictional grips. The displacement of the grips was monitored with a Linear Voltage Displacement Transmitter (LVDT) that has a detection limit below 1 μm displacement. The shear stress is measured as load divided by the solder-substrate contact area (total area of the wetted pads). The shear strain (simple shear) is the relative displacement of the sample plates divided by solder joint thickness. Creep tests were conducted until steady state was reached and passed, and the reported creep rates were the steady-state creep rates. Samples were tested at 3 different temperatures: 60°C, 95°C and 130°C, and at 5 different load levels at each temperature.

## III. Creep behavior

The microstructures of the four solders are illustrated in Fig. 3(a-d). The Sn-3.5Ag, Sn-3Ag-0.5Cu and Sn-0.7Cu solders have microstructures that consist of large islands of nearly pure Sn divided by regions that are decorated with $Ag_3Sn$ or $Cu_6Sn_5$. Both precipitate phases were found in Sn-3Ag-0.5Cu. The Sn-10In-3.1Ag solder is a mixture of intermetallic phases. Metallographic estimates are in at least rough agreement with the published ternary phase diagram [6], whose 100°C isothermal section suggests a mixture of 74% InSn (γ), 22% Sn (β), and 4% $Ag_2In$. Increasing the cooling rate from 3.5°C/min. to 2.7°C/sec. produced somewhat finer microstructures in all alloys, without much apparent change in the geometric features.

Figure 4(a-c) shows creep curves for the Sn-3Ag-0.5Cu solder joints, and Fig. 5(a-c) shows the corresponding curves for the Sn-10In-3.1Ag alloy. The smooth load-displacement curves shown in Fig. 4 are typical for the Sn-Ag and Sn-Cu solders. There is a fairly rapid evolution into a well-defined steady behaves in a similar manner, but the load-displacement curves tend to be more noisy, particularly at 95°C.

Steady state strain rates were measured as functions of stress and temperature from the linear portions of the creep curves for the four solder compositions and for identical joints of pure Sn. Log-log plots of the steady-state strain rates as functions of stress for the solder joints are given in Fig. 6(a-d). The data are ordinarily fit to constitutive equations of the Dorn form [7]:

$$\dot{\gamma} = \frac{AGb}{kT}\left[\frac{\tau}{G}\right]^n \exp\left[\frac{-Q}{kT}\right] \qquad (1)$$

where $\dot{\gamma}$ is the shear strain rate, $\tau$ the shear stress, G the shear modulus, b the Burgers vector, Q the activation energy and kT the Boltzmann temperature. If this is done, the data divide naturally into high- and low-stress regions with different stress exponents (n), as is often found for solder joints [1].

The major anomaly in the data is in the temperature dependence of the stress exponent in the high-stress regime. The stress exponent in the high-stress regime is

greater than about 7 in all cases, but increases dramatically as the temperature is decreased from 95°C to 60°C, a range of significant technological interest. The fact that this behavior is common to all of the Sn-rich solders suggests that it is due to the Sn-rich constituent itself. This is illustrated in Fig. 7(a,b) which compares the steady state creep rates of the solder joints to that of pure Sn joints at 60°C and 95°C. The steady-state creep behavior of Sn-0.7Cu is almost identical to that of pure Sn over this stress range. The more highly alloyed SnAg and SnAgCu solders are more creep-resistant than Sn, but have almost identical stress exponents at the two temperatures. It certainly appears that the anomalous temperature dependence of the Sn-rich solders is primarily due to the behavior of Sn itself.

Surprisingly, the SnInAg solder has a creep behavior very like that of the SnAg and SnAgCu solders, despite the fact that its predominant phase is hexagonal γ-InSn rather than tetragonal Sn. It is not clear whether the similar creep behavior of this alloy is due to similarities in the behavior of γ-InSn and β-Sn, or to the possibility that β-Sn dominates despite its smaller volume fraction. We know of no creep data on γ-InSn.

Given the anomalous temperature dependence of the stress exponent it is deceptive to use the conventional Dorn equation to represent the creep data. There is no well-defined activation energy at lower temperatures; the activation energy depends on the stress at which it is measured.

Nonetheless, a force-fit to the Dorn equation may be useful as a first-order fit to the creep behavior over this temperature regime. For this reason the best-fit stress-exponents and activation energies are tabulated in Table 1, and compared with those for pure Sn. The best-fit activation energies cluster about 85 kJ/mole, the measured value for pure Sn. The SnInAg alloy is exceptional, having apparent activation energies above about 100 kJ/mole (this may reflect the dominant volume fraction of γ-InSn in this alloy). The best-fit stress exponents in the low-stress regime vary from near 3 (SnCu) to 6.6 (SnAgCu). However, note the anomaly in the low-stress behavior of the SnInAg alloy (Fig. 6d); for reasons that are unclear, the low-stress behavior was not detected in tests at 130°C. The best-fit stress exponents in the high-stress regime are much higher, ranging from 7.7 (Sn) to 10.7 (SnAgCu).

The quality of the fit to the Dorn equation is illustrated by Fig. 8, which is typical for the data taken here. A superficial study of this plot suggests that the Dorn equation is quite reasonable. It is only when the data for the several alloys is separated by temperature that the systematic deviation from this equation becomes apparent.

Finally, Fig. 9 illustrates the influence of the cooling rate after reflow. Increasing the cooling rate softens the solder (raises the strain rate at given stress) without significantly changing the stress exponent. This softening in creep is a common consequence of grain refinement which, among other effects, increases the contribution of grain boundary sliding to the creep rate.

## VI. Discussion

The data presented here suggest that the creep behavior of Sn-rich solders is dominated by the behavior of Sn, and has an anomalous temperature dependence at temperatures slightly above room temperature. While the literature on the creep of pure Sn is not entirely consistent, there are indications of thermal anomalies in several

published reports. In particular, Breen and Weertman [9], Suh, et al. [10], and Poirier [11] all noted significant changes in the creep behavior of bulk Sn at about 100°C, evidenced by a change in the activation energy for steady-state creep from above 100 to below 50 kJ/mole. Frenkel, et al. [12] and Mohamed, et al. [13] confirm the high-temperature value of the activation energy, while Adeva, et al. [14], Mathew, et al. [15] and others [16,17] have measured much lower activation energies at lower temperature. The measured activation energies are close to those for lattice diffusion (~100 kJ/mole [18,19]) and dislocation pipe diffusion (40-60 kJ/mole [14,20,21]) suggesting that the dominant activation step changes from lattice to pipe diffusion as the temperature drops.

While the change in creep behavior with temperature complicates the understanding and prediction of creep in Sn-rich solders, the relative insensitivity of the creep behavior to composition simplifies it. Eutectic Sn-0.7Cu is very close to Sn in its creep behavior, while the addition of Ag hardens the solder without dramatically changing the stress exponents or activation energies, that is, the predominant effect is on the pre-exponential factor, A, in eq. (1). The addition of 0.5Cu to Sn-3Ag does not significantly change the creep behavior.

Surprisingly, the addition of 10In to Sn-3Ag does not change the creep behavior dramatically, either, even though it does change the dominant phase. This behavior is not understood, and needs further investigation.

The stress exponents reported in the literature for Sn and Sn-rich solders scatter widely, from near 5 (Breen and Weertman [9], Darveaux and Banerji [22]) to 10-11 (Yang, et al. [23], Mavoori, et al. [24]). In the present work, this whole range of stress exponents appears in the same data set, depending on the stress range and the temperature. In particular, the data reported here show a systematic change in stress exponent with stress and temperature for all of the solders studied. It is not yet clear to what extent this systematic variation explains the wide variations in reported results.

The data presented in Fig. 8 and Table 1 show that while thermal anomalies in the creep behavior were found at temperatures near 100°C, these anomalies were not obviously associated with a change in activation energy of the sort reported from prior work. They were rather associated with changes in the stress exponent. We do not yet know why this is the case, but it may be significant that changes in the stress exponent alter the measured activation energy by an amount that depends on the precise value of stress that is used to measure the activation energy. The error is particularly large if the reference stress is chosen so that the high-temperature data fall in the high-stress regime while the low-temperature data fall in the low-stress regime.

Finally, we should note the tetragonal crystal structure of Sn, which causes anisotropy in its mechanical properties. The creep behavior of Sn and Sn-rich joints may, therefore, be affected by crystallographic texture, particularly in as-solidified solder joints. The crystallographic texture of the joints studied here is not yet known.

## V. Conclusion

The creep behavior of Sn and Sn-rich solder joints in shear is a complex function of stress and temperature. In particular, the stress exponent that governs steady-state creep has different values in the low- and high-stress regimes. The stress exponent at high stress changes significantly with temperature as temperature drops below about

100°C, and reaches anomalously high values (n = 10-11) at lower temperatures. These anomalous features suggest that qualification and design verification tests for Sn-rich solder joints should use geometries and conditions as near as possible to those anticipated in service, until further research clarifies how this complex creep behavior can be understood metallurgically and treated analytically.

## Acknowledgments

This research was supported by Intel Corporation and by the Director, Office of Science, Office of Basic Energy Sciences, Division of Materials Sciences and Engineering, of the U.S. Department of Energy under Contract No. DE-AC03-76SF00098.

## List of References

1. J.W. Morris, Jr. and H.L. Reynolds: *Design and Reliability of Solders and Solder Interconnections*, ed. by R.K. Mahidhara, D.R. Frear, S.M.L. Sastry, K.L. Murty, P.K. Liaw and W. Winterbottom, (TMS Soc., Warrendale, PA, 1997) pp. 49-58.
2. M.C. Shine and L.R. Fox: *Low Cycle Fatigue, ASTM STP 942*, ed. by H.D. Solomon, G.R. Halford, L.R. Kaisand and B.N. Leis, (ASTM, Philadelphia, PA, 1988) pp. 588-610.
3. K. Suganuma: MRS Bulletin **26** (2001) 880-884.
4. H.G. Song, J.W. Morris, Jr. and M.T. McCormack: J. Electron. Mater. **29** (2000) 1038-1046.
5. J.L.F. Goldstein and J.W. Morris, Jr.: J. Electron. Mater. **23** (1994) 477-486.
6. I. Ohnuma, Y. Cui, X.J. Liu, Y. Inohara, S. Ishihara, H. Ohtani, R. Kainuma and K. Ishida: J. Electron. Mater. **29** (2000) 1113-1121.
7. J.E.Bird, A.K. Mukherjee and J.E. Dorn: *Quantitative Relation Between Properties and Microstructure*, ed. by D.G. Brandon and A. Rosen, (Israel University Press, Jerusalem, 1969) pp. 255-342.
8. Z. Guo, Y-H Pao and H. Conrad: J. Electron. Packag. **117** (1995) 101-104.
9. J.E. Breen and J. Weertman: Trans. AIME: **203** (1955) 1230-1234.
10. S.H. Suh, J.B. Cohen and J. Weertman: Metall. Trans. A **14A** (1983) 117-126.
11. J.P. Poirier: Acta Metall. **26** (1978) 629-637.
12. R.E. Frenkel, O.D. Sherby and J.E. Dorn: Acta Metall. **3** (1955) 470-472.
13. F.A. Mohamed, K.L. Murty and J.W.Morris, Jr.: Metall. Trans. **4** (1973) 935-940.
14. P. Adeva, G. Caruana, O.A. Ruano and M. Torralba: Mater. Sci. Eng. A **A194** (1995) 17-23
15. M.D. Mathew, S. Movva, H. Yang and K.L. Murty: *Creep Behaviors of Advanced Materials for the 21st Century*, ed. by R.S. Mishra, A.K. Mukherjee and K.L. Murty, (TMS Soc., Warrendale, PA, 1999) pp. 51-59.
16. L. Rotherham, A.D.N. Smith and G.B. Greenough: J. Inst. Met. **79** (1951) 439-454.
17. R. J. McCabe and M. Fine: JOM **52** (2000) 33-35.
18. J.D. Meakin and E. Klokholm: Trans. Met. Soc. AIME **218** (1960) 463-466.
19. C. Coston and N.H. Nachtrieb: J. Phys. Chem. **68** (1964) 2219-2229.

20. V.I. Igoshev and J.I. Kleiman: J. Electron. Mater. **29** (2000) 244-250.
21. T. Reinikainen and J. Kivilahti: Metall. Mater. Trans. A **30A** (1999) 123-132.
22. R. Darveaux and K. Banerji: IEEE Trans. Comp. Hybrids, Manuf. Technol. **15** (1993) 1013-1024.
23. H. Yang, P. Deane, P. Magill and K.L. Murty: *Proc. 46th Electr. Comp. Technol. Conf.,* (IEEE, New York, NY, 1996) pp. 1136-1142.
24. H. Mavoori, J. Chin, S. Vaynman, B. Moran, L. Keer and M. Fine: J. Electron. Mater. **26** (1997) 783-790.

**List of Captions for Table and Figures**

Table 1. The best-fit stress exponents (n) and activation energies (Q) for creep of solder joints. The temperature dependence of the shear modulus of pure Sn in ref. 8 was used for the data analysis of all solder joints.

Figure 1. Schematic diagram of the specimen geometry.
Figure 2. Schematic diagram of creep test machine.
Figure 3. Cross-sectional optical micrographs of solder joints with composition (a) Sn-3.5Ag, (b) Sn-3Ag-0.5Cu, (c) Sn-0.7Cu and (d) Sn-10In-3.1Ag.
Figure 4. Creep Curves of Sn-3Ag-0.5Cu at (a) 60°C, (b) 95°C and (c) 130°C.
Figure 5. Creep Curves of Sn-10In-3.1Ag at (a) 60°C, (b) 95°C and (c) 130°C.
Figure 6. Log-log plots of the steady-state strain rate as a function of stress for the solder joints with composition (a) Sn-3.5Ag, (b) Sn-3Ag-0.5Cu, (c) Sn-0.7Cu and (d) Sn-10In-3.1Ag.
Figure 7. The steady-state strain rates of all alloy solder joints and pure Sn joints at (a) 60°C and (b) 95°C.
Figure 8. Typical log-log plots of $(d\gamma/dt)(T/G)\exp(Q/kT)$ versus $\tau/G$. G(T) (MPa) = 16302 – 40.5 T (°C) for pure Sn [8] was used for the analysis.
Figure 9. The influence of the cooling rate on creep at 130°C in Sn-0.7Cu and Sn-3Ag-0.5Cu solder joints.

Table 1. The best-fit stress exponents (n) and activation energies (Q) for creep of solder joints. The temperature dependence of the shear modulus of pure Sn in ref. 8 was used for the data analysis of all solder joints.

| Solders | n | | Q (KJ/mole) | |
|---|---|---|---|---|
| | Low $\tau/G$ | High $\tau/G$ | Low $\tau/G$ | High $\tau/G$ |
| Sn | 5.8 | 7.7 | 85 | 65 |
| Sn-Ag | 4.5 | 10.6 | 80 | 75 |
| Sn-Ag-Cu | 6.6 | 10.7 | 95 | 75 |
| Sn-Cu | 3.5 | 8.9 | 90 | 85 |
| Sn-In-Ag | 5.4 | 9.5 | 100 | 115 |

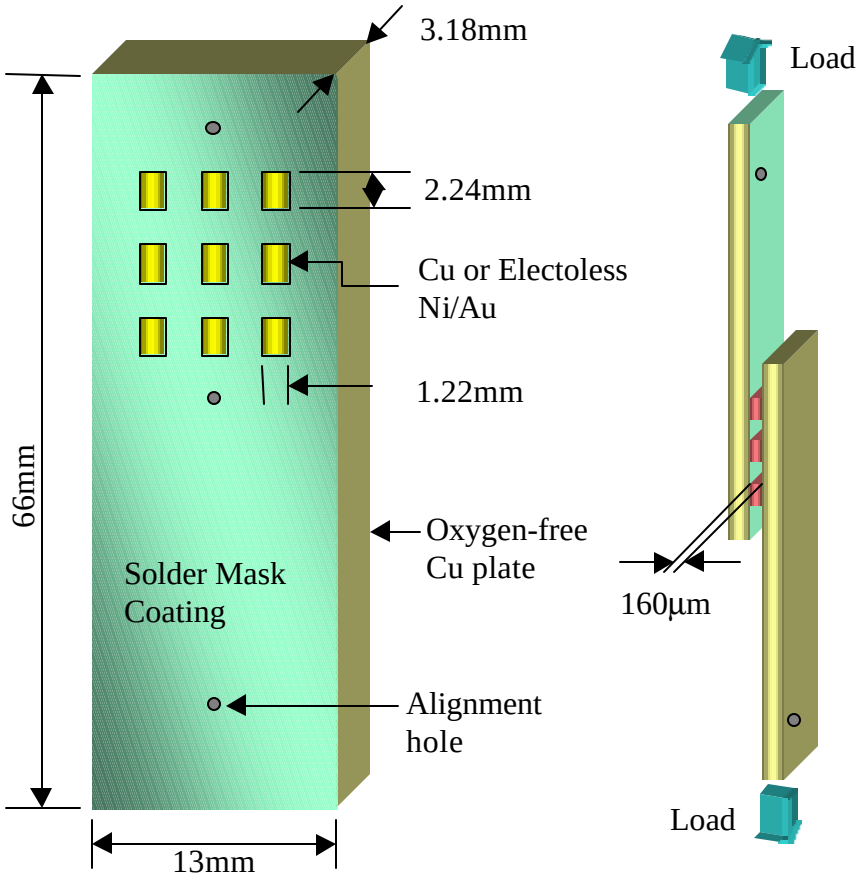


Figure 1. Schematic diagram of the specimen geometry.

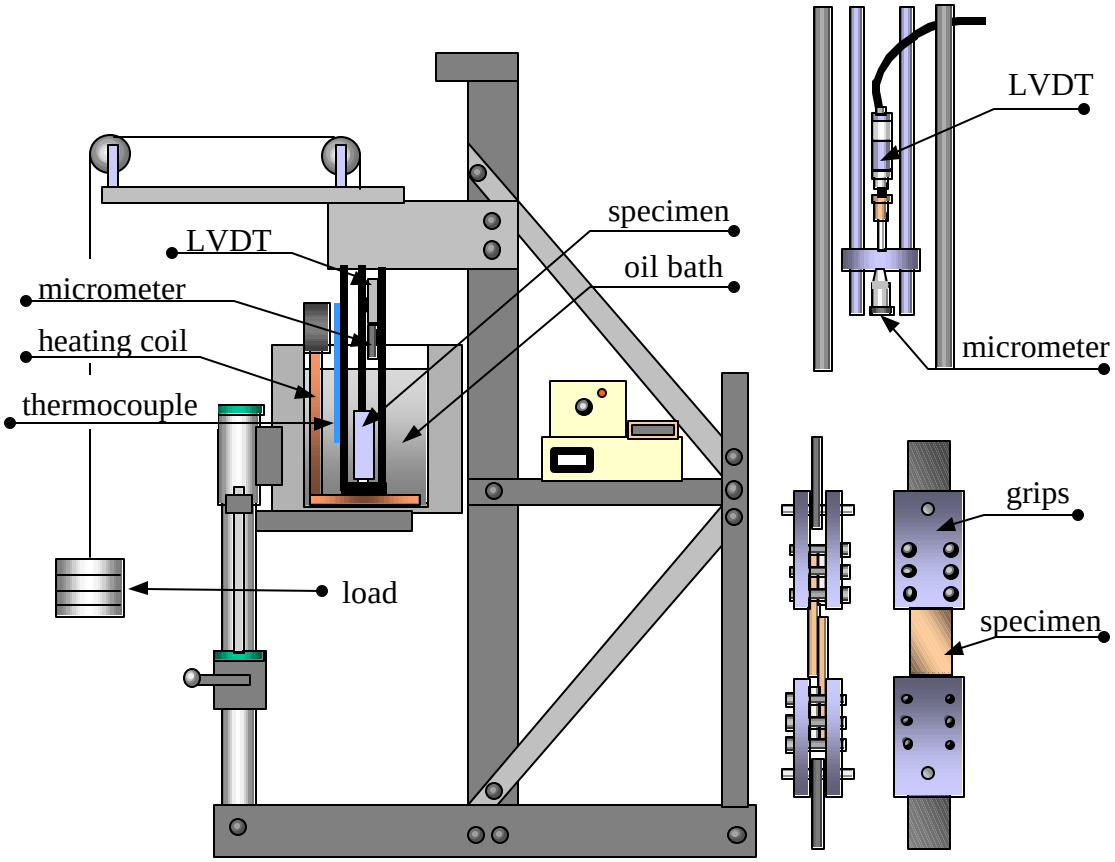


Figure 2. Schematic diagram of creep test machine.

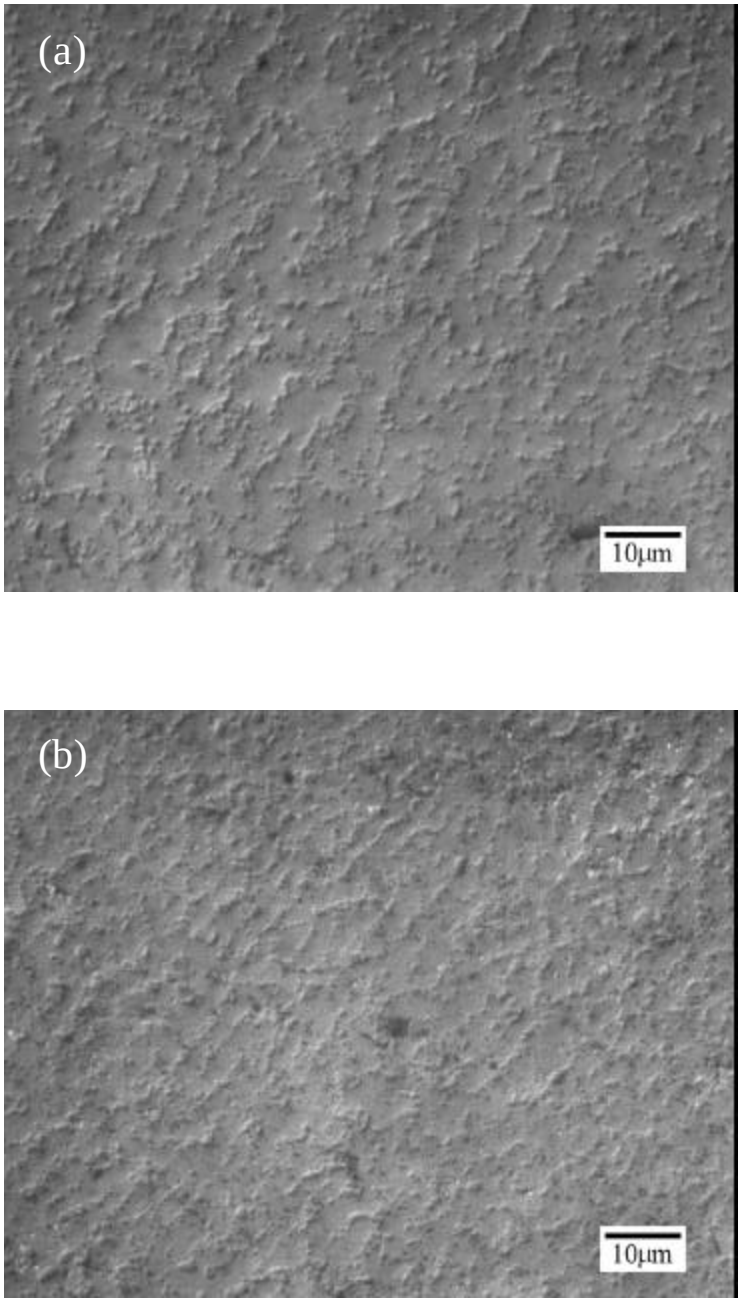


Figure 3. Cross-sectional optical micrographs of solder joints with composition (a) Sn-3.5Ag, (b) Sn-3Ag-0.5Cu, (c) Sn-0.7Cu and (d) Sn-10In-3.1Ag.

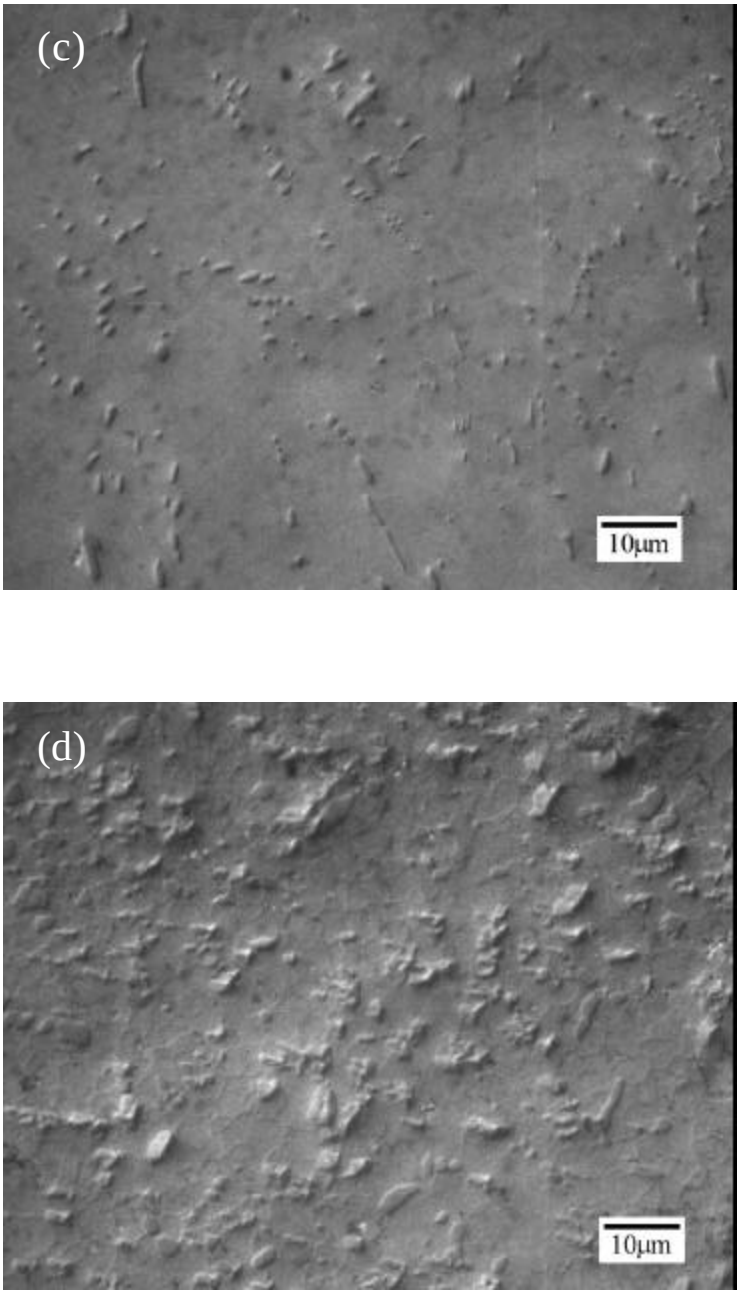


Figure 3. Cross-sectional optical micrographs of solder joints with composition (a) Sn-3.5Ag, (b) Sn-3Ag-0.5Cu, (c) Sn-0.7Cu and (d) Sn-10In-3.1Ag.

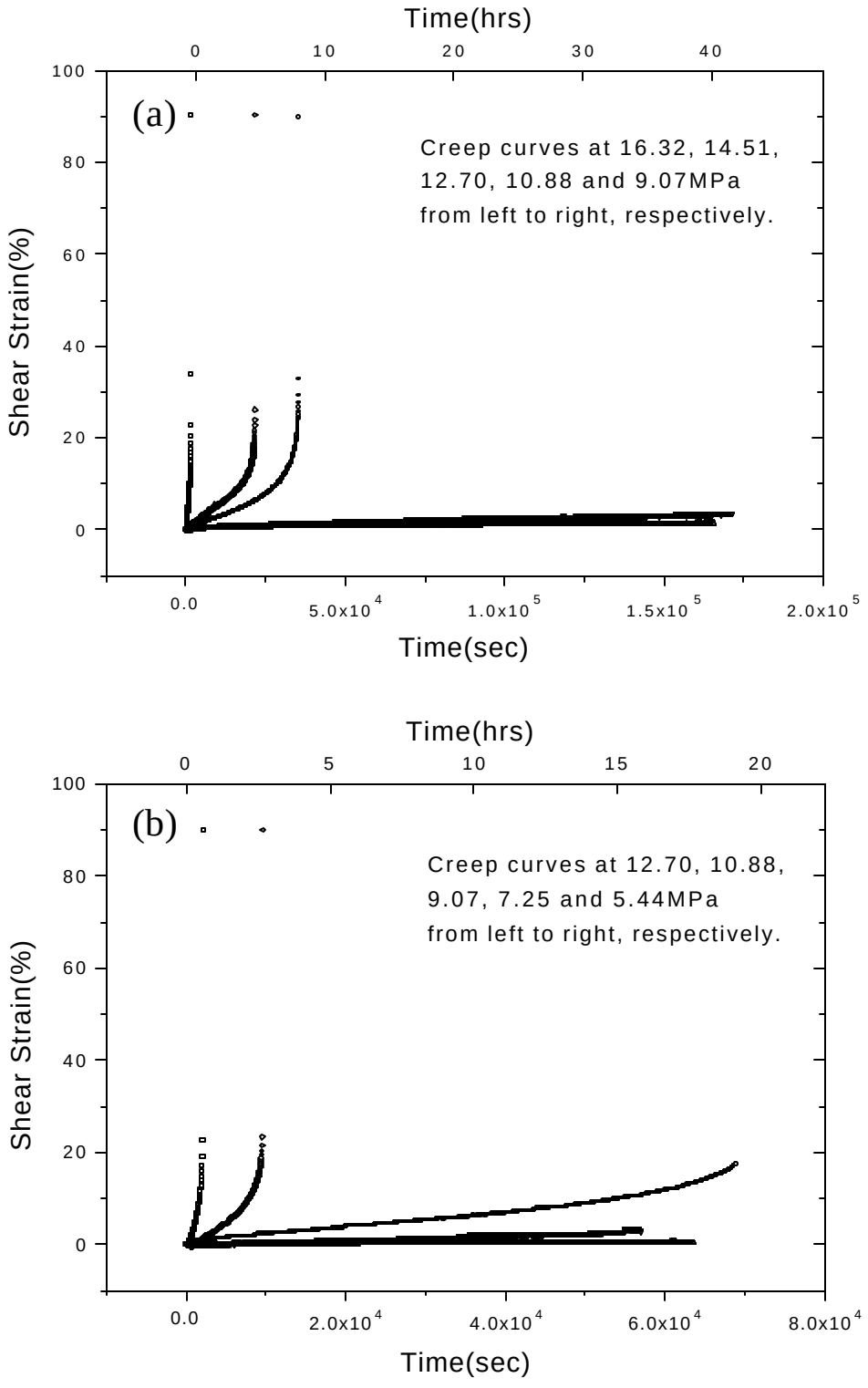


Figure 4. Creep Curves of Sn-3Ag-0.5Cu at (a) 60°C, (b) 95°C and (c) 130°C.

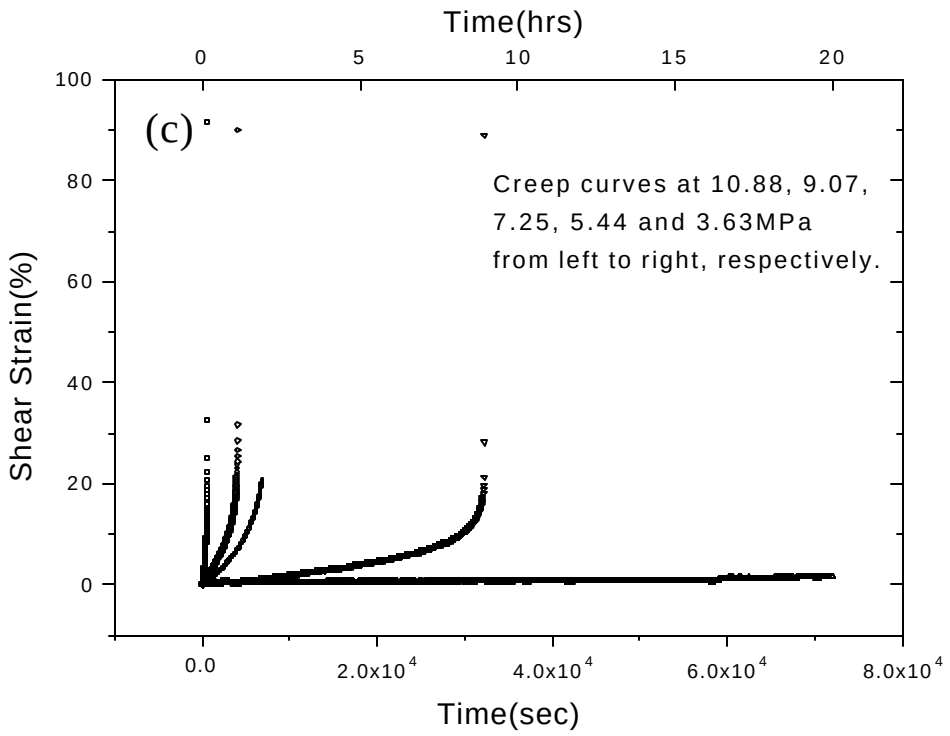


Figure 4. Creep Curves of Sn-3Ag-0.5Cu at (a) 60°C, (b) 95°C and (c) 130°C.

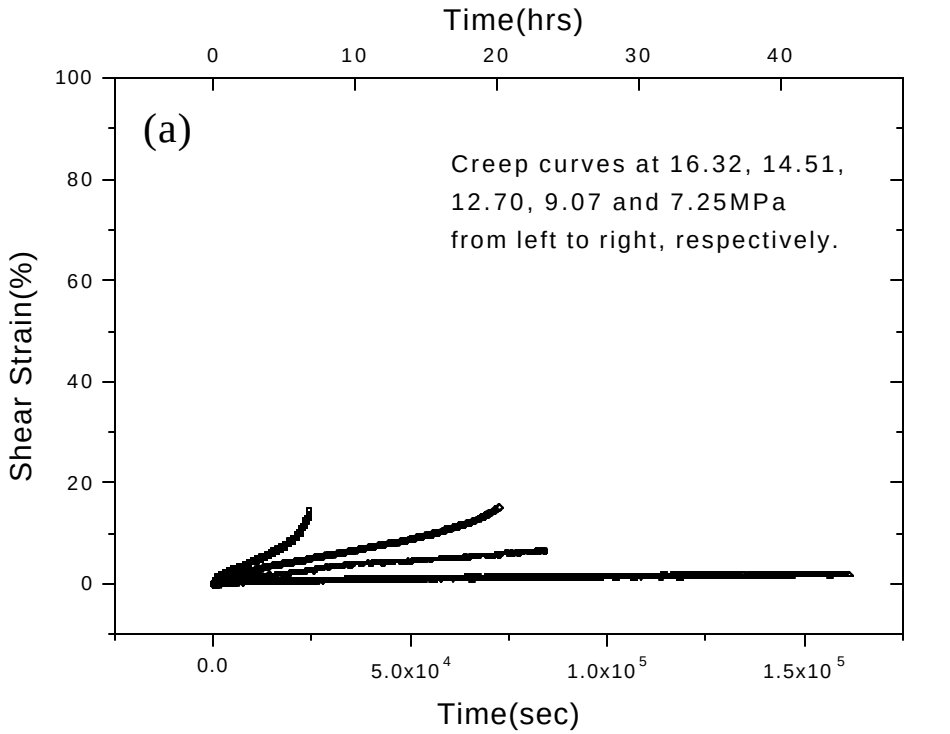


Figure 5. Creep Curves of Sn-10In-3.1Ag at (a) 60°C, (b) 95°C and (c) 130°C.

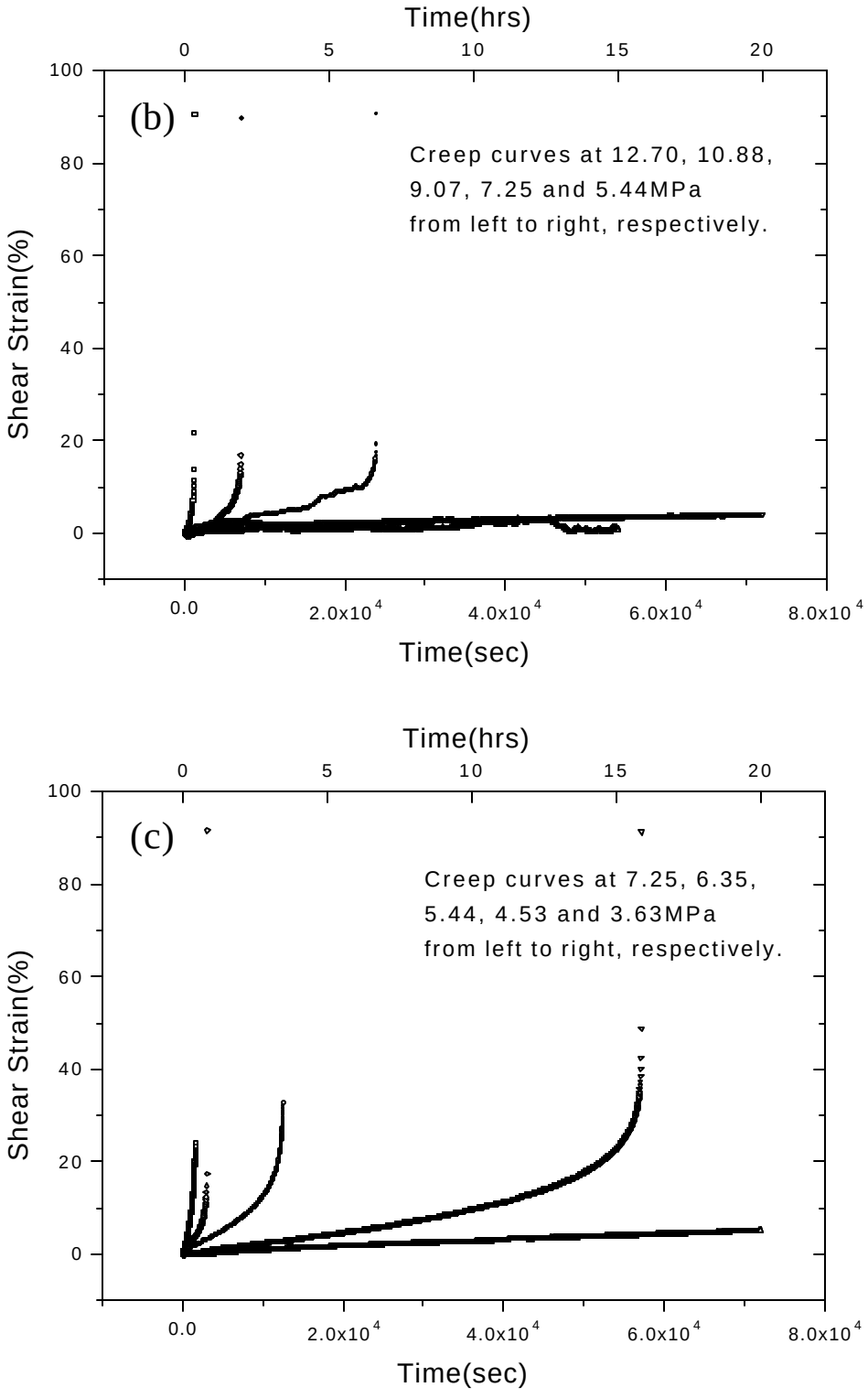


Figure 5. Creep Curves of Sn-10In-3.1Ag at (a) 60°C, (b) 95°C and (c) 130°C.

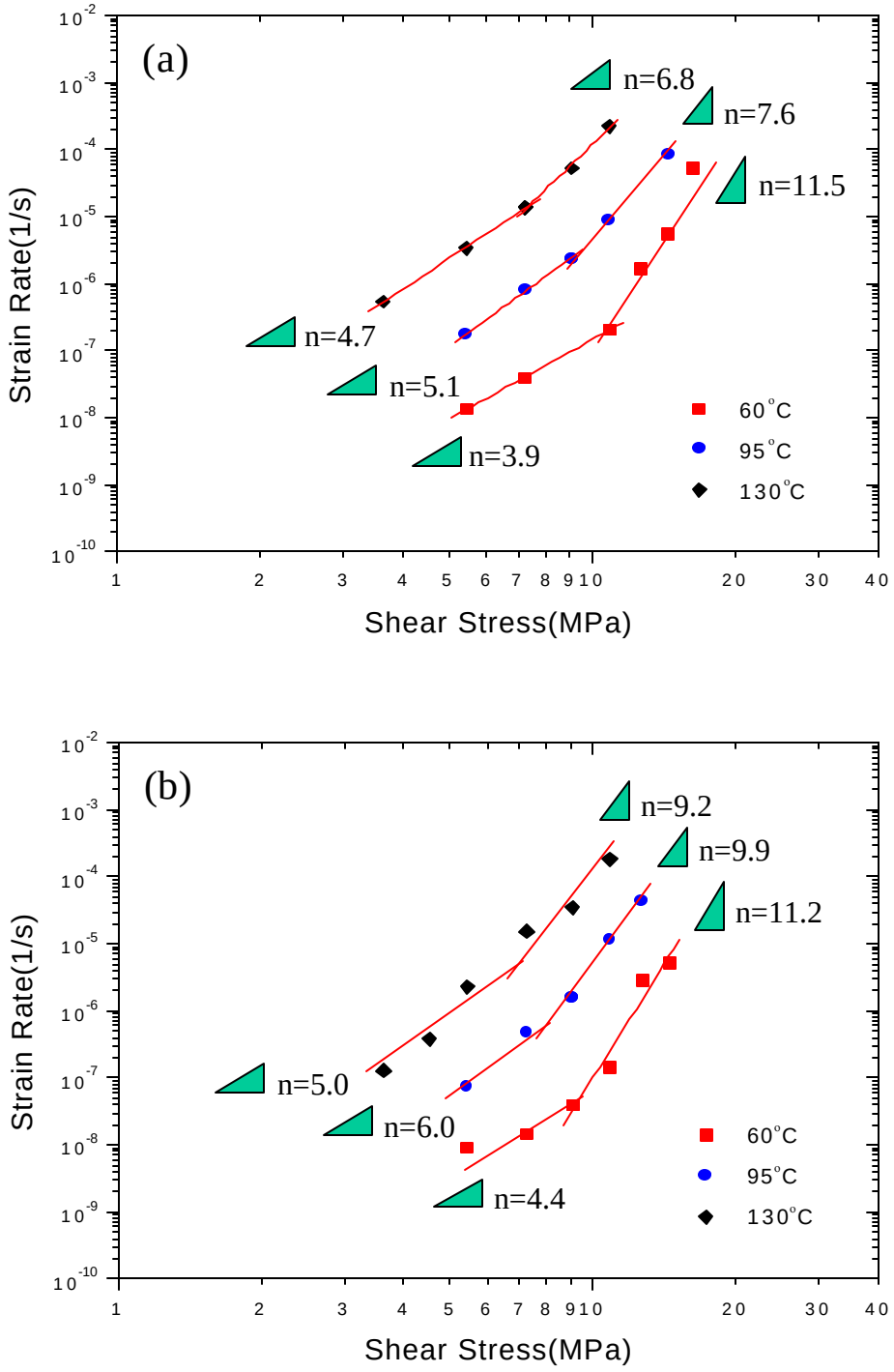


Figure 6. Log-log plots of the steady-state strain rate as a function of stress for the solder joints with composition (a) Sn-3.5Ag, (b) Sn-3Ag-0.5Cu, (c) Sn-0.7Cu and (d) Sn-10In-3.1Ag.

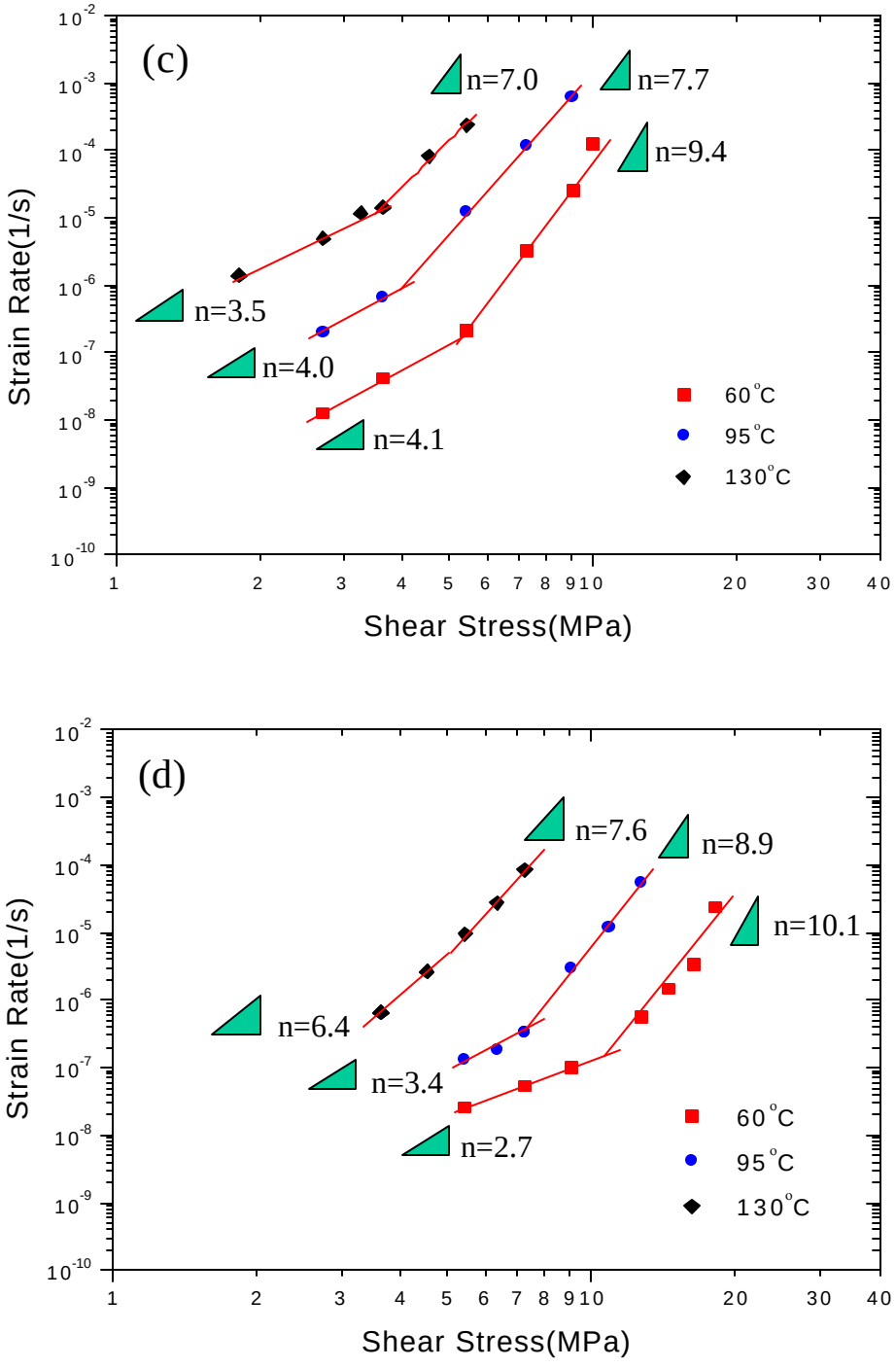


Figure 6. Log-log plots of the steady-state strain rate as a function of stress for the solder joints with composition (a) Sn-3.5Ag, (b) Sn-3Ag-0.5Cu, (c) Sn-0.7Cu and (d) Sn-10In-3.1Ag.

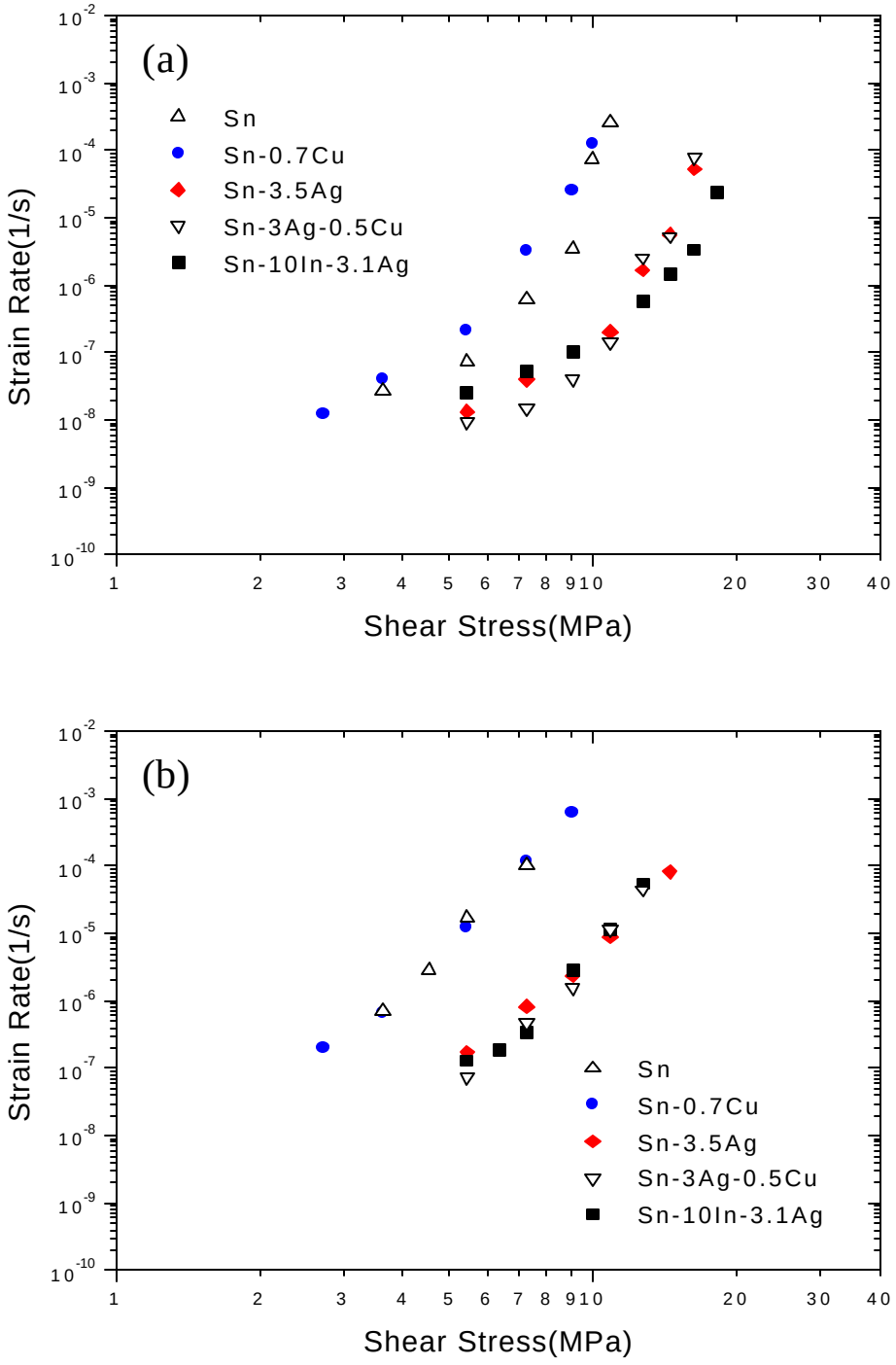


Figure 7. The steady-state strain rates of all alloy solder joints and pure Sn joints at (a) 60°C and (b) 95°C.

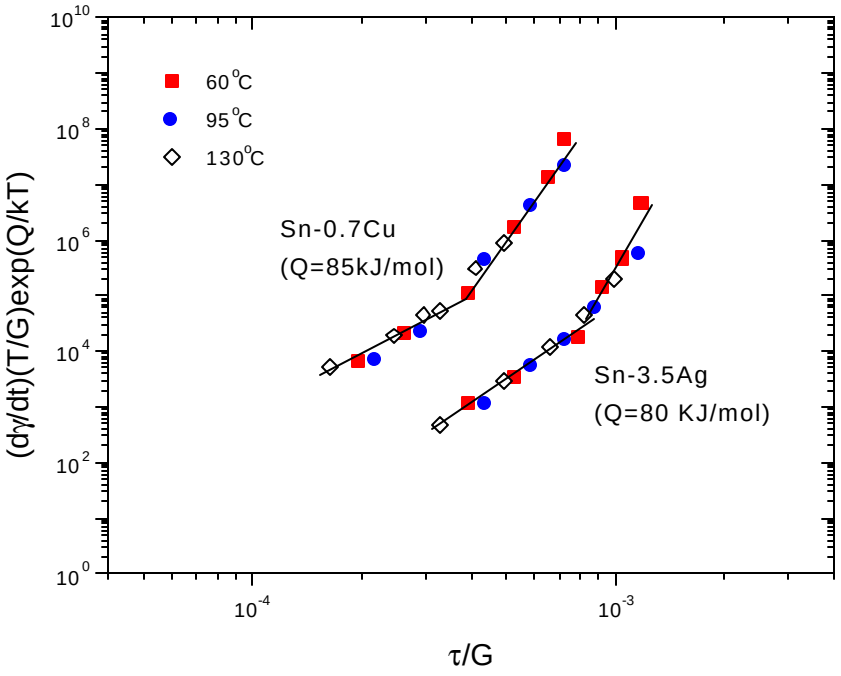


Figure 8. Typical log-log plots of (dγ/dt)(T/G)exp(Q/kT) versus τ/G. G(T) (MPa) = 16302 – 40.5 T (°C) for pure Sn [8] was used for the analysis.

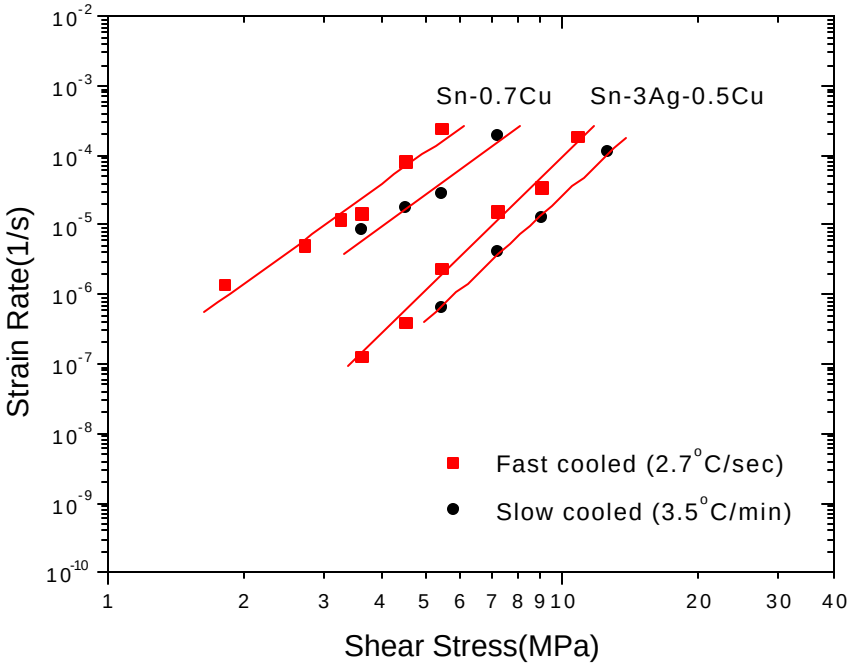


Figure 9. The influence of the cooling rate on creep at 130°C in Sn-0.7Cu and Sn-3Ag-0.5Cu solder joints.